Cell

Evolution of Resistance to a Last-Resort Antibiotic in *Staphylococcus aureus* via Bacterial Competition

Gudrun Koch,[1] Ana Yepes,[1] Konrad U. Förstner,[2] Charlotte Wermser,[1] Stephanie T. Stengel,[1] Jennifer Modamio,[1] Knut Ohlsen,[2] Kevin R. Foster,[3,4] and Daniel Lopez[1,2,*]
[1]Research Centre for Infectious Diseases (ZINF), University of Würzburg, Würzburg 97080, Germany
[2]Institute for Molecular Infection Biology (IMIB), University of Würzburg, Würzburg 97080, Germany
[3]Department of Zoology
[4]Oxford Centre for Integrative Systems Biology
University of Oxford, Oxford OX1 3QU, UK
*Correspondence: daniel.lopez@uni-wuerzburg.de
http://dx.doi.org/10.1016/j.cell.2014.06.046

SUMMARY

Antibiotic resistance is a key medical concern, with antibiotic use likely being an important cause. However, here we describe an alternative route to clinically relevant antibiotic resistance that occurs solely due to competitive interactions among bacterial cells. We consistently observe that isolates of Methicillin-resistant *Staphylococcus aureus* diversify spontaneously into two distinct, sequentially arising strains. The first evolved strain outgrows the parent strain via secretion of surfactants and a toxic bacteriocin. The second is resistant to the bacteriocin. Importantly, this second strain is also resistant to intermediate levels of vancomycin. This so-called VISA (vancomycin-intermediate *S. aureus*) phenotype is seen in many hard-to-treat clinical isolates. This strain diversification also occurs during in vivo infection in a mouse model, which is consistent with the fact that both coevolved phenotypes resemble strains commonly found in clinic. Our study shows how competition between coevolving bacterial strains can generate antibiotic resistance and recapitulate key clinical phenotypes.

INTRODUCTION

Antibiotics are the primary treatment for bacterial infections. However, the number of effective antibiotics is decreasing due to the rising numbers of multi-drug-resistant pathogens. The path to resistance generally involves the acquisition of specific mutations that enable bacteria to grow in the presence of the antibiotics recommended for their treatment (Cantón and Morosini, 2011). However, the development of antibiotic resistance is also a naturally occurring process in bacteria, which is not exclusively restricted to clinically relevant species (Benveniste and Davies, 1973). For example, bacteria in the environment may secrete antibiotics to remove niche competitors. These bacteria themselves harbor genes enabling them to resist their own antimicrobials (Allen et al., 2010), and in turn, they exert a selective pressure on neighboring bacteria to acquire mutations or transferred genes that are protective (Hibbing et al., 2010). This raises the possibility that the rising levels of antibiotic resistance in pathogens may also be influenced by competitive microbial interactions, similar to what occurs in natural environments.

Multi-drug-resistant strains are becoming more and more prevalent in the hospital environment, and as a consequence, they are increasingly responsible for nosocomial infections. One of the most threatening hospital-associated pathogens is the bacterium *Staphylococcus aureus*, which currently represents a major problem in both the clinical and community settings. However, *S. aureus* is not exclusively a pathogen and commonly colonizes the nasopharynx and skin (Kluytmans et al., 1997). Nevertheless, most of these strains have the capacity to cause severe infections when associated with bones and soft tissues, which occasionally progress to life-threatening diseases such as necrotizing fasciitis or pneumonia (Otto, 2012). Moreover, due to the widespread use of the antibiotic methicillin in the 1960s, several strains exist that are resistant to a wide range of β-lactam antibiotics, known as methicillin-resistant *S. aureus* or MRSA (Kreiswirth et al., 1993). MRSA infections are difficult to treat, with a mortality rate of ~20%, and are the leading cause of death by a single infectious agent in the USA, being responsible for more deaths than HIV (Klevens et al., 2007). More recently, a subset of community-associated MRSA (CA-MRSA) strains has emerged that, in addition to being resistant to multiple antibiotics, is no longer restricted to clinical settings and has the ability to cause severe and pandemic infections in healthy individuals (Diep et al., 2008). The traditional approach to treat MRSA and CA-MRSA infections has been the glycopeptide vancomycin, and therefore, it is a common treatment for staphylococcal infections. However, the general use of the antibiotic has led to the emergence of several strains that display reduced susceptibility to vancomycin (Hiramatsu et al., 1997). These strains are commonly referred to as vancomycin-intermediate *S. aureus* (VISA), and although their level of

resistance is relatively moderate (MIC = 4–8 μg/ml) in comparison to strains that are fully resistant to vancomycin (vancomycin resistance *S. aureus*, VRSA) (MIC ≥ 16 μg/ml), due to their prevalence, VISA strains represent a major threat to overcoming staphylococcal infections (Howden et al., 2010).

The antibacterial activity of vancomycin relies on its capacity to bind to and inactivate certain precursors of cell wall synthesis, which exclusively localize at the division septum in *S. aureus* (Pereira et al., 2007). *S. aureus* strains acquire intermediate resistance to vancomycin treatment via the acquisition of point mutations in regulatory genes that lead to the thickening of the cell wall. This provides a protective barrier against the diffusion of vancomycin to its target at the division septum (Howden et al., 2010; Pereira et al., 2007). VISA strains emerge from vancomycin-susceptible strains during infections treated with the antibiotic (Hiramatsu et al., 1997), and in contrast to the rare cases of VRSA infections, VISA strains cause numerous difficult-to-treat, hospital-associated infections. However, it is also puzzling that VISA strains have been detected in patients with renal failure or a prosthetic joint that have not been treated with vancomycin (Charles et al., 2004; Howden et al., 2010). These infections are usually associated with high-cell-density bacterial colonization, which is currently considered one of the risk factors that promotes the occurrence of VISA (Charles et al., 2004; Howden et al., 2010).

Bacterial colonization at high cell density involves prolonged periods of infection and the formation of surface-associated aggregates or biofilms (López et al., 2010). Biofilm formation is a key feature of staphylococcal infections, in addition to the secretion of virulence factors (Herbert et al., 2010). The *agr* quorum-sensing (QS) system of *S. aureus* controls the infection process by upregulating virulence factors, such as membrane-disrupting toxins (Hla, Hlb, and Hlg), proteases, lipases, enterotoxins, superantigens, and urease while at the same time indirectly downregulating the extracellular matrix and adhesin proteins responsible for cell aggregation and biofilm formation (Boles and Horswill, 2008; Peng et al., 1988; Recsei et al., 1986). Importantly, *agr* is repressed by the σ^B stress-induced sigma factor. σ^B is activated during biofilm formation in response to cellular stress and triggers the expression of a general stress response regulon that includes genes associated with pigmentation and biofilm formation (Bischoff et al., 2001; Kullik et al., 1998).

A growing body of empirical and theoretical work suggests that biofilm-encased cells are subjected to strong natural selection, as they compete for space and nutrients, which can shape microbial phenotypes and diversity (Nadell et al., 2009). These conditions give rise to a heterogeneous population of genetically different bacteria that display characteristics that are relevant to understanding the progression of an infection. We hypothesized that a biofilm environment of a single staphylococcal clone could be a factor shaping the diversity of MRSA strains in which the pathogen could evolve new phenotypes that resist antibiotic treatment. This report presents evidence for an unexpected route to the evolution of antibiotic resistance in staphylococcal communities that occurs without the selective pressure of antibiotic treatment but solely via intraclonal competitive interactions between bacterial cells. Microbial aggregates of a single staphylococcal isolate spontaneously evolved new competitive phenotypes in a coevolutionary arms race that ultimately led to the emergence of an intermediate resistant phenotype similar to VISA clinical isolates. Our study provides evidence for how bacterial interactions play an important role in microbial evolution and may serve to explain the diversification of key clinical phenotypes.

RESULTS

Strain Diversification in Staphylococcal Biofilms

The genetic basis of biofilm formation in *S. aureus* has been routinely explored using submerged surfaces in tryptone soy broth (TSB) medium + NaCl 500 mM (Beenken et al., 2003; Götz, 2002). However, to study the diversification and evolution of new strains, we established a biofilm formation assay in *S. aureus* using solid agar (Branda et al., 2001). The assay utilized Mg^{2+}-enriched conditions because previous studies have shown that chronic staphylococcal infections due to biofilm formation occur in niches contain a high concentration of Mg^{2+} (e.g., joints or bones) (Günther, 2011; Jahnen-Dechent, 2012), whereas tissues unintentionally depleted of Mg^{2+} are prone to acute staphylococcal infections (Schlievert, 1985). *S. aureus* strains were grown on TSB + 100 mM $MgCl_2$ solid agar (tryptone soy broth supplemented with magnesium, TSBMg) for 5 days. After incubation, staphylococcal communities developed into robust aggregates with a complex architecture in which immobilized cells became encased within an extracellular matrix, as reported for other species (Branda et al., 2001; Serra et al., 2013) (Figures 1A, S1A, and S1B available online). When extending this assay to clinical isolates, we observed morphological diversity (Figure S1C), and a number of strains (SC01, RN1, N315, LAC, and HG003 strains) reproducibly developed distinct sectors that were phenotypically different to the parental strain as the colonies grew across the plate (Figures 1A and S1C) (Servin-Massieu, 1961). The development of the distinct sectors is consistent with the appearance of *S. aureus* variants that display a competitive advantage during growth.

To gain insight into the evolution of these new variants and their potential roles in biofilm formation during clinically relevant infections, we focused on a CA-MRSA clinical isolate (SC01 derivative) that displayed the most evident sectoring phenotype among all strains tested. The wild-type (WT) strain initially formed an orange-colored center region or origin (O). The orange color comes from the carotenoid pigment staphyloxanthin, which is responsible for the golden coloration of *S. aureus* (Marshall and Wilmoth, 1981). Over time, a second unpigmented strain emerged that is white (W) and rapidly surrounded the origin. Subsequently, a third strain emerged, forming yellow flares (Y) that radiated from the origin and through the white sector to generate a distinctive flower-like distribution pattern of cells within the bacterial community (Figures 1B and S1D). Diversification of W and Y phenotypes strongly depended on the presence of Mg^{2+} in the medium and occurred in both liquid culture and solid agar biofilm assays (Figures S1E and S2A).

When isolated and reinoculated, O cells developed a similar distribution of alternating sectors of nonpigmented and pale yellow pigmented cells. However, isolation and reinoculation of W and Y cells resulted in a homogeneous community (Figure 1B). In addition to the differences in pigmentation, O cells displayed an increased ability to form biofilms in the conventional biofilm

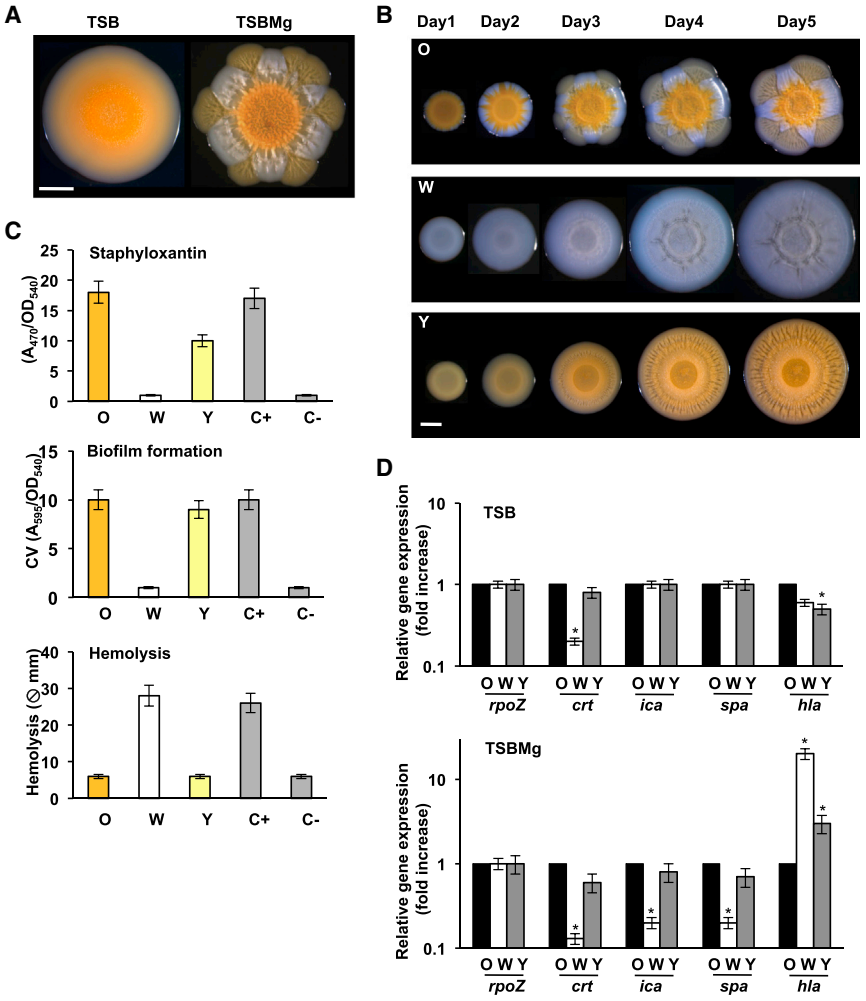

Figure 1. Strain Diversification in Communities of *S. aureus*

(A) *S. aureus* SC01 derivative strain grown in TSB and TSBMg for 5 days at 37°C.

(B) Progression of O, W, and Y strains when growing in TSBMg for 5 days at 37°C. Scale bars, 1 mm.

(C) Measurements of Staphyloxanthin production, biofilm formation, and secretion of hemolytic toxins in O, W, and Y strains. C+ is LAC strain, and C- is LAC $\Delta\sigma^B$ mutant. Hemolysis efficiency used LAC $\Delta\sigma^B$ mutant as a C+, and C- is LAC strain.

(D) qRT-PCR of the expression staphyloxanthin production (*crt*), biofilm formation (*ica* and *spa*), and hemolytic toxins (*hla*) in O, W, and Y strains in TSB and TSBMg growing media (Student's t test, $p \leq 0.05$).

See Figures S1 and S2.

formation assay and a low ability to secrete hemolytic toxins (Figure 1C). W cells showed the opposite biological activities and Y cells displayed an intermediate response in the collection of assays that we performed. Furthermore, quantitative RT-PCR (qRT-PCR) analyses verified that these differences were associated with changes in expression of key genes involved in these processes (Figures 1D and S2B). Pigment production, biofilm formation, and hemolysis directly correlated with the expression of staphyloxanthin (*crt*) (Pelz et al., 2005), biofilm-related genes (*ica* and *spa* genes) (O'Gara, 2007; Otto, 2008), and hemolytic toxin genes (*hla*) (Brown and Pattee, 1980), respectively, suggesting that O, W, and Y strains are physiologically distinct.

W Strain Displays a Hyperactive QS Phenotype

The phenotypic characterization of the initial O strain displaying increased biofilm production and decreased toxin secretion suggested that the QS system was repressed because *agr* QS system activates the expression of secreted toxins and inhibits genes involved in biofilm formation. Yet, the decreased biofilm formation and increased toxin secretion in W suggested that the *agr* pathway had become active (see Figure 2B). The differential activation of the QS system was explored by the global gene expression profiling using RNA-sequencing (RNA-seq) for the O, W, and Y strains (Figure S3A and Table S3). Comparison of the O and W gene expression signatures revealed hyperactivated expression of the *agr* QS system in W compared to O (Figures 2A and S3B), which occurred concomitantly with enhanced expression of a number of *agr*-regulated genes. Activation of QS in W is associated with hyperproduction of the autoinducing peptidic pheromone (AIP). At the threshold concentration, AIP binds to its membrane-bound receptor AgrC and triggers a QS response in *S. aureus* (Novick and Geisinger, 2008; MDowell et al., 2001; Thoendel et al., 2011). We genetically engineered a synthetic *Bacillus subtilis* strain to express a fluorescent AIP-responsive reporter (Figures S3C–S3G). Diluted supernatants of O, W, and Y strains were added to cultures of the *B. subtilis* reporter strain. Supernatants from W contained more AIP than those from O or Y (Figure 3A).

The phenotypic and transcriptional changes found in the W strain were consistent with a σ^B loss-of-function mutation. The stress-induced sigma factor σ^B strongly represses *agr* and induces staphyloxanthin production (Bischoff et al., 2001; Kullik et al., 1998), which would explain the high-expression *agr* and the lack of pigmentation in W strain (Figure 2B). To test this, we used qRT-PCR analysis to monitor two *agr*-dependent RNAII and RNAIII transcripts (Novick and Geisinger, 2008; Thoendel et al., 2011). RNAII and RNAIII were highly expressed in the W strain compared with the O strain, which is consistent with increased *agr* expression in W (Figure 3B). RNAII activates the *agrBDCA* operon that encodes the *agr* regulatory cascade (Bischoff et al., 2001, 2004), which regulates the expression of the surfactant phenol-soluble modulins (PSMs) (Queck et al., 2008). RNAIII activates *agr*-dependent genes such as *hla* (Morfeldt et al., 1995, 1996) (Figure 2B). Consistent with a σ^B-deficient phenotype, both *psms* and *hla* were highly expressed in

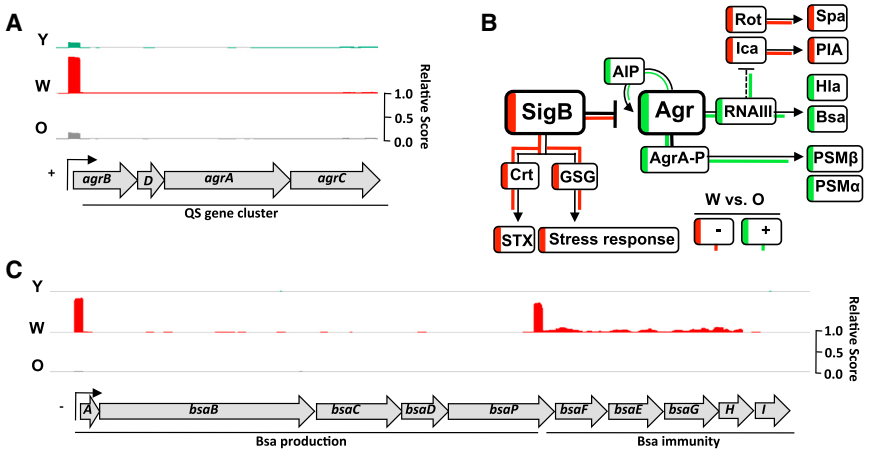

Figure 2. Correlation of Genome-wide Gene Expression Levels Quantified by RNA-Seq

(A) Read coverage of the *agr* gene cluster in O, W, and Y. The expression of *agr* in W is increased ~20-fold in relation to O.

(B) Schematic overview of the genetic circuitry that antagonistically regulates toxin secretion and biofilm formation in *S. aureus*. Arrows are positive regulation, and T bars are repression. Dashed line is indirect regulation. Staphyloxanthin production is STX, and GSG are general stress genes. Transcriptional activation in W is represented in green, and downregulation is represented in red.

(C) Read coverage of the *bsa* gene cluster in O, W, and Y cells. The expression of the *bsa* in W strain is increased ~300-fold in relation to O strain.

See Figure S3 and Tables S3, S4, and S5.

the W strain (Figure 3B). We therefore searched for adaptive mutations that would produce a σ^B-deficient phenotype by sequencing the *sigB* operon (*rsbU-rsbV-rsbW-sigB*) (Figure S4A) in nine different W strains derived from three independent evolution experiments. In each case, we found key point mutations in an essential residue for the kinase activity of the RsbW antisigma factor (Figures S4A, ii, and S4B). RsbW binds to and prevents σ^B binding to the RNA polymerase. RsbW is also sequestered by RsbV. Phosphorylation of RsbV by RsbW releases RsbW to bind to and inhibit σ^B (Marles-Wright and Lewis, 2010) (Figure S4A). The mutation in RsbW inhibits its binding to RsbV, generating a nonfunctional σ^B complex with RsbW (Dufour and Haldenwang, 1994), possibly targeting it for degradation (Graham et al., 2013) (Figures S4C and S4D).

QS upregulates the production of secondary metabolites, including antibiotics and PSMs surfactants (Table S4). This included increased production of antibiotics that inhibited the growth of O strain (see below) and PSMs surfactants that enabled W to efficiently expand and rapidly colonize the plates in a spreading assay (Figure 3C) (Tsompanidou et al., 2013) and also in the biofilm formation assay (Figure 3E). The PSMs were responsible for the increased spreading (Figures S4E–S4G). Complementation of a σ^B-deficient laboratory strain with the σ^B operon from W strains did not restore the WT phenotype, which was rescued only by the σ^B operon from the O strain (Figure S4H). To demonstrate the evolutionary advantage of QS hyperactivation in W, we purified the AIP signal that triggers QS in *S. aureus* from W cultures and added to the growth medium of the O strain (MDowell et al., 2001). Activation of QS in W is associated with hyperproduction of the AIP. Under these conditions, the W or Y phenotypes were not observed (Figure 3D). To summarize, W arises through a mutation that inhibits σ^B and causes hyperactivation of QS, enabling the strain to both spread from and inhibit the growth of the parental strain.

W Strain Produces Bsa Bacteriocin that Selects for the Evolution of the Y Strain

To provide evidence for a growth advantage of W over O, a growth assay was performed using a tractable CA-MRSA strain (LAC) as a proxy O strain and a Δ*sigB* mutant as W strain. The WT and Δ*sigB* strain were combined in a 5:1 ratio and grown in TSBMg (5:1 is the empirically determined O:W ratio observed upon initiation of diversification; Figure S2A). After incubation, the synthetic communities recreated the phenotype previously observed in the CA-MRSA colonies, with the WT strain restricted to the origin and the QS-high strain (Δ*sigB* strain) rapidly expanding and forming a white ring surrounding the colony (Figure 3E). Thus, hyperactivation of the *agr* QS in the σ^B-deficient strain provided a growth advantage over the WT strain, enabling it to rapidly spread. Importantly, the third yellow phenotype strain that was not present in the original mixture also evolved during the time course of the experiment. This third yellow strain radiated from the WT sector in the center and grew through the σ^B-deficient strain sector, similar to behavior of the Y phenotype of the original CA-MRSA colonies.

The emergence of the Y strain after the W strain suggests that the presence of W may be important for the evolution of Y strain. As described above, phenotypic and transcriptomic data revealed that the W strain produced several extracellular active compounds. We detected high expression of a CA-MRSA-associated gene cluster responsible for the production of the lantibiotic Bsa (bacteriocin of *S. aureus*) and its resistance machinery (Figures 2C and S3B). Antibiotic-producing bacteria use antibiotics to remove niche competitors, and Bsa enables CA-MRSA to compete with the natural flora of healthy individuals and facilitates the growth of CA-MRSA when coexisting with other bacteria (Daly et al., 2010), thus indicating the potential of Bsa to act as a selective pressure in the evolution of microbes.

Expression analysis of σ^B-deficient strain revealed an increase in *bsa* expression, which was also dependent on *agr* (Kies et al., 2003). As expected, W also showed higher expression of *bsa*-related genes compared to O and Y (Figure 4A). Next, supernatants of O, W, and Y cultures were tested for antimicrobial activity against *B. subtilis* (Figures 4B and 4C). Supernatants from W inhibited *B. subtilis* growth. Likewise, supernatants from σ^B-deficient strains were toxic, and this toxicity was attenuated in the absence of the *agr* or *bsa* gene clusters (Figures 4B and 4C).

The above experiments confirmed that the W strain produced more Bsa antibiotic than O and Y strains (Table S4 and S5), but it was unclear whether Bsa was responsible for the selective

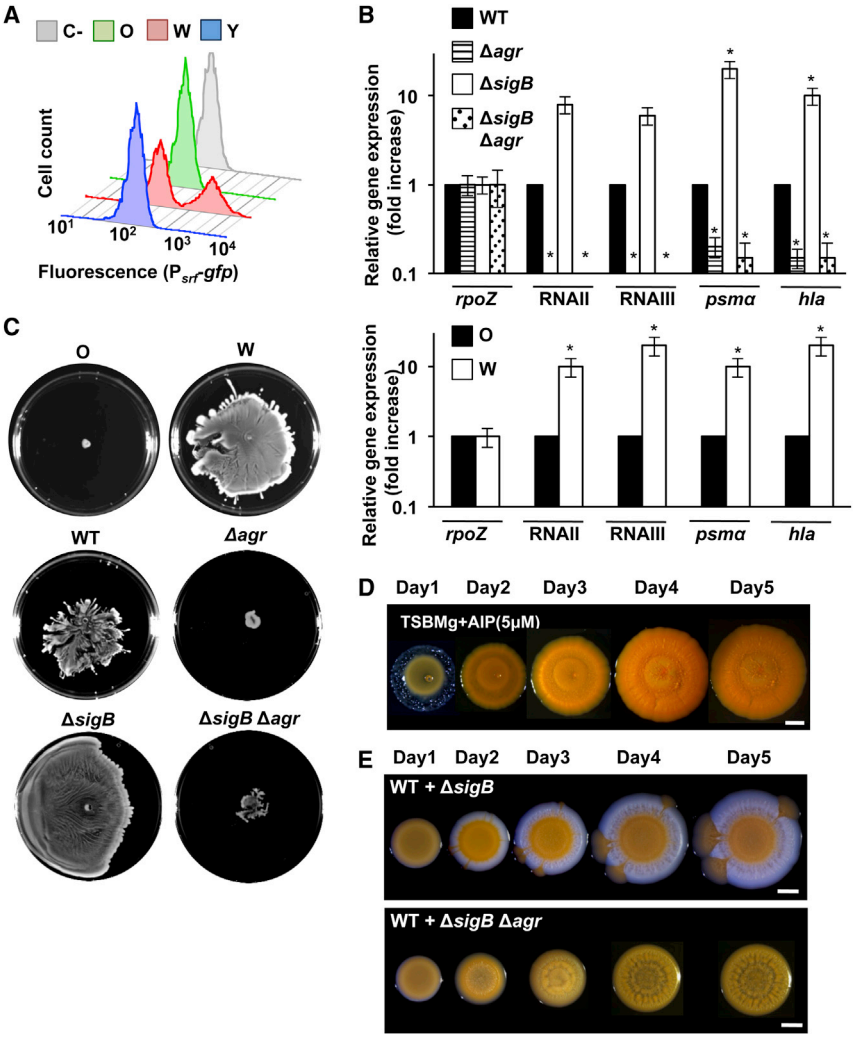

Figure 3. Adaptive Abilities of the W Strain

(A) Quantification of AIP in O, W, and Y supernatants using a *B. subtilis* transducer strain and monitored by flow cytometry (n = 50,000 events). Gray profile is control with no supernatant added.

(B) qRT-PCR analysis of RNAII, RNAIII, and regulated genes in different genetic backgrounds (Student's t test, $p \leq 0.05$).

(C) Spreading assay to monitor the ability of distinct strains to expand on solid surfaces. Samples were spotted and incubated for 24 hr at 37°C. Multicellular communities of distinct strains growing in TSBMg for 5 days at 37°C.

(D) Complementation of TSBMg with 5 μM AIP. Plates were incubated at 37°C for 5 days.

(E) Synthetic communities of different strain mixtures (ratio 5:1) were spotted in TSBMg and incubated at 37°C. Y_A strain differentiates after 5 days of incubation. Scale bars, 1 mm.

See Figures S3, S4, and S6.

pressure to generate the Y genotype. Addition of exogenous Bsa to O, W, and Y cultures in TSB liquid medium strongly inhibited the growth of O. Importantly, the addition of Bsa did not affect the growth of W and minimally affected the growth of Y (Figure 4D, top row). Furthermore, in the synthetic mixed populations (described above), deletion of the *bsa* cassette in a σ^B-deficient strain did not prevent the rapid expansion of the σ^B-deficient strain but prevented the emergence of the Y strain (Figure 5A, top row). Likewise, the Y strain did not evolve from an O strain lacking the *bsa* cluster (Figure 5B). Importantly, the addition of exogenous Bsa to the O strain (grown on TSBMg agar) bypassed the requirement for the W phenotype and Y flares directly evolved from a growth-restricted O community in the absence of W sectors (Figure 5A, bottom row). These results suggest an important role for Bsa in the evolution of the Y phenotype.

Y Strain Shows a VISA-like Phenotype that Tolerates the Presence of Bsa

Similar to many other antibiotics, Bsa is an epidermin-like antibiotic that targets lipid II during bacterial cell wall synthesis. Vancomycin also inhibits cell wall synthesis by binding to the D-Ala-D-Ala residues in the lipid-II-linked pentapeptide precursor of peptidoglycan (lipid-II-AA) (see Figure S7A) (Howden et al., 2010). Vancomycin has been consistently used to treat MRSA infections. However, recently, the emergence of strains that are intermediate resistant to vancomycin (VISA) (Hiramatsu et al., 1997), as well as other cell wall antibiotics, has been observed (Camargo et al., 2008; Peleg et al., 2012). VISA strains display increased cell wall thickening, which reduces the access of vancomycin to its lethal target (lipid-II-AA) at the division septum (Figures S7A and S7B). Interestingly, we find that most sequenced VISA strains derived from susceptible parental strains that do not contain the *bsa* gene cluster (Figures S5A and S5B), which is similar to what is seen in VRSA (Kos et al., 2012). Thus, the acquisition of the VISA phenotype potentially enables Bsa-defective strains to tolerate the presence of Bsa in mixed communities (Figure S5C) because it has been recently reported that ~30% of staphylococcal infections involves colonization by multiple strains (Votintseva et al., 2014).

We explored the possibility that Y cells have acquired a VISA-like phenotype to tolerate the presence of Bsa. Addition of vancomycin to Y cultures revealed intermediate resistance (IR) to vancomycin similar to their IR to Bsa (Figure 4D, bottom row). In contrast, IR to vancomycin was not detected in W cultures, which indicated that the VISA phenotype was specific to Y strains. There are multiple pathways by which cells can acquire a VISA phenotype. Nevertheless, mutations in *graRS*, *vraRS*, and *walKR* two-component systems have been consistently found in VISA isolates (Hafer et al., 2012; Howden et al., 2010). To detect the existence of mutations that may confer a VISA-like phenotype to Y, we performed a whole-genome sequence

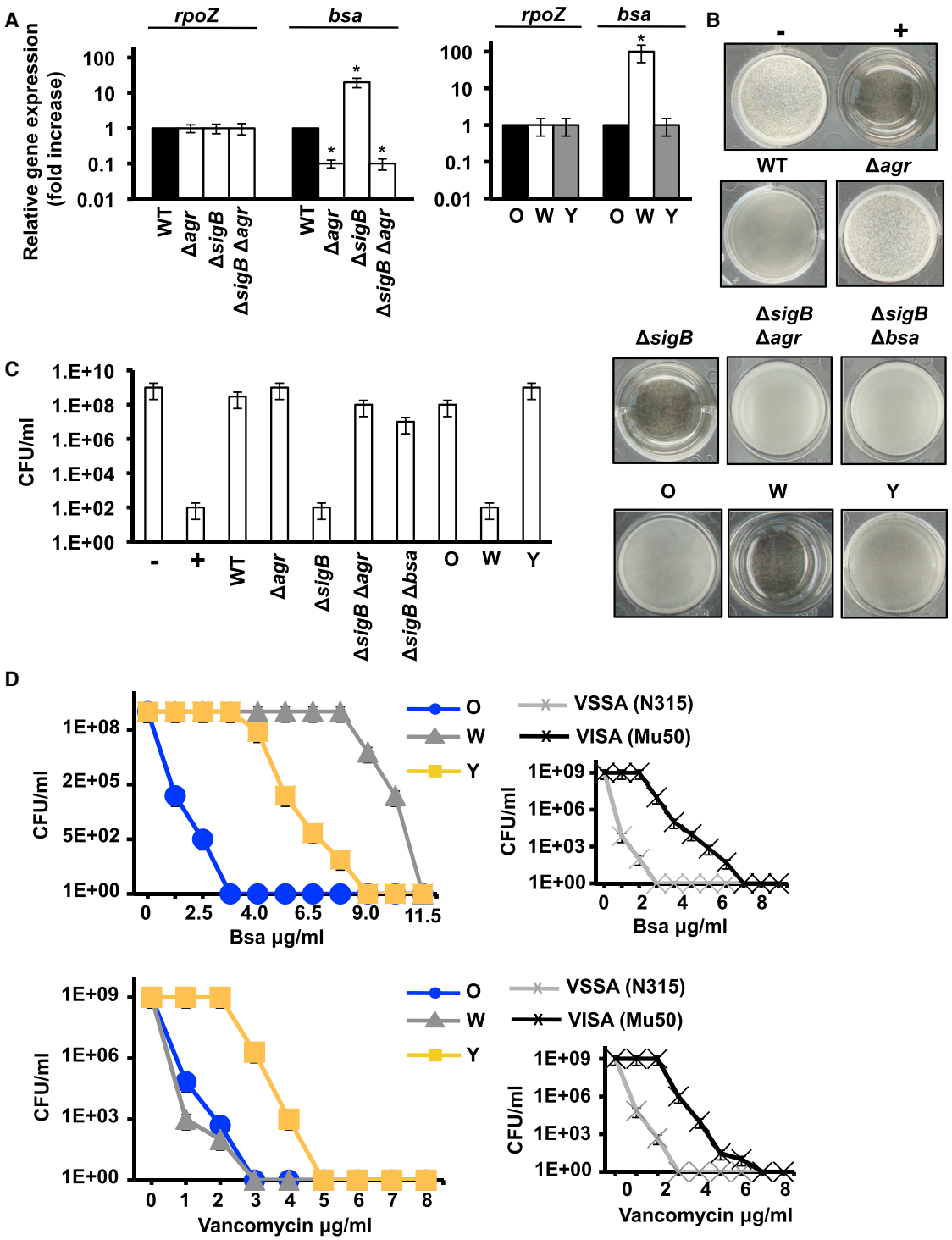

Figure 4. Adaptive Abilities of the Y Strain

(A) qRT-PCR analysis of the expression of *bsa* in distinct genetic backgrounds (Student's t test, $p \leq 0.05$).

(B) Antimicrobial activity of filter-sterilized supernatants. 50 µl was used to supplement 1 ml cultures of *B. subtilis*. Growth inhibition prevented biofilm growth. Negative and positive controls (– and +) represent *B. subtilis* cultures without and with kanamycin 5 µM.

(C) Quantification microbial survival (CFU/ml) in *B. subtilis* cultures conditioned with Bsa.

(D) Growth curves of O, W, and Y in TSB medium with different concentrations of Bsa or vancomycin (CFU/ml). Right panels show control growth curves of isogenic VSSA/VISA strains (N315/Mu50) in the presence of different concentrations of Bsa or vancomycin.

See Figure S5.

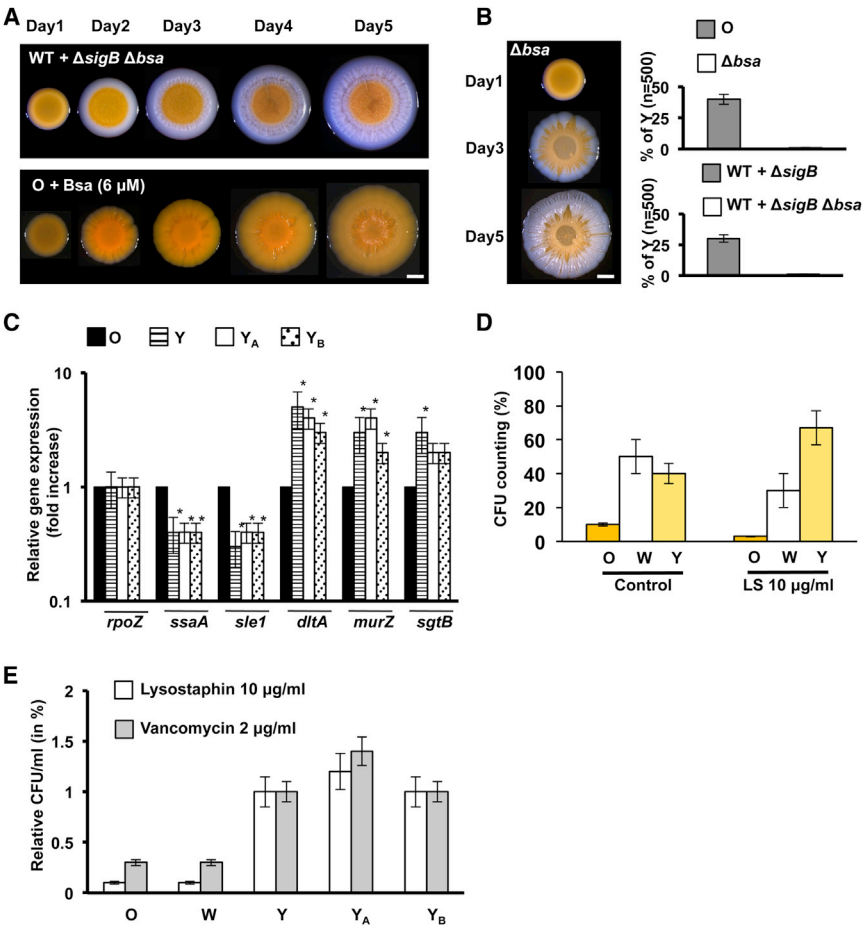

Figure 5. Y Strain Is a VISA-like Strain

(A) Progression of mixed LAC WT strain + LAC Δ*sigB* Δ*bsa* mutant in relation 5:1 (top). The communities grew in TSBMg at 37°C for 5 days. After incubation, the community failed to develop Y flares through the W sector. Progression of the O strain in TSBMg at 37°C for 5 days when supplemented with previously purified Bsa (~6 μM) (lower row). Y_B strain differentiates. Scale bar, 1 mm.

(B) Progression of the O strain Δ*bsa* mutant in TSBMg at 37°C for 5 days. After incubation, the community failed to develop Y flares through the W sector.

(C) qRT-PCR analysis of several VISA-related genes (*ssaA*, *sle1*, *dltA murZ*, and *sgtB*) in O, Y strains and Y_A and Y_B strains derived from the artificial mixture WT+Δ*sigB* (Figure 3G) and Bsa supplementation (Figure 5A), respectively (Student's t test, $p \leq 0.05$).

(D) Quantification of bacterial survival in response to lysostaphin treatment (LS 10 μg/ml for 15 min at 37°C).

(E) Quantification of bacterial survival in response to lysostaphin and vancomycin treatment of different strains in relation to Y strain.

See Figures S5 and S7 and Table S6.

comparison between Y and O. This revealed mutations in the GraRS and WalKR two-component systems (Figure S6B), which were further confirmed by Sanger sequencing of nine independent evolutionary events in different colonies. Importantly, amino acid substitutions detected in these two-component systems have been previously described in VISA isolates (Matsuo et al., 2013). The *agr* operon was sequenced as a control to confirm that no mutations occurred in this locus. In addition, the Y strains that evolved from the experiments of mixed communities (Y_A strain shown in Figure 3E) or after exposure to Bsa (Y_B strain shown in Figure 5A) were also sequenced. VISA-like mutations were also found in the *graRS*, *vraRS*, and *walKR* operons in both strains (Figure S6B).

GraRS, VraRS, and WalKR synergistically regulate a number of genes involved in cell-wall synthesis. This stimulon is permanently activated in VISA strains, which results in cell wall thickening that reduces the access of vancomycin to its lethal target lipid-II-AA at the division septum (Howden et al., 2010) (Figures S7A and S7B). Gene expression analyses of VISA-related genes confirmed the upregulation of cell-wall genes and downregulation of autolysins in the different Y strains (Figures 5C and S5D). Reduced diffusion of vancomycin to the septum was confirmed in Y cells coupled to a thickening of the cell wall using electron microscopy (Figures S7C–S7E) and reduced membrane susceptibility to the endopeptidase lysostaphin (Sieradzki and Tomasz, 2003) (Figure 5D). In addition to this, the Y_A and Y_B strains were more tolerant to the action of lysostaphin than W cells and were comparable to the natural Y strain (Figure 5E). As expected, Y_A and Y_B strains showed IR to vancomycin similar to the Y strain, suggesting a VISA-like phenotype (Figure 5E). Complementation of a VSSA laboratory strain with the *graRS*, *vraRS*, and *walKR* operons from different Y strains also resulted in IR to vancomycin (Figure S5D). In sum, the production of Bsa by W drives the evolution of the Y strain, which bears a striking similarity to VISA isolates that have been described in the clinics.

O, W, and Y Strains Also Evolve in In Vivo Infections

The emergence of two phenotypes from a MRSA isolate in vitro demonstrates that clinically relevant properties can evolve solely via competitive interactions within an MRSA colony biofilm. However, it was unclear whether such biofilm-associated evolutionary events could drive similar diversification in an in vivo infection situation. Based on our in vitro data, we predicted that regions of the body that are efficiently colonized by *S. aureus* (cut-off $\geq 10^5$ colony forming units [CFU]/g of organ) (Table S7) would coincide with the reservoirs of magnesium of the body (i.e., bones and kidneys) (Günther, 2011; Jahnen-Dechent, 2012), which would favor biofilm-like growth and the emergence of the W and Y strains. Hence, a cohort of five mice was infected with 10^7 CA-MRSA cells that were previously grown in the absence of Mg^{2+} to prevent strain diversification (Figure S2A). After 5 days of infection, mice were sacrificed

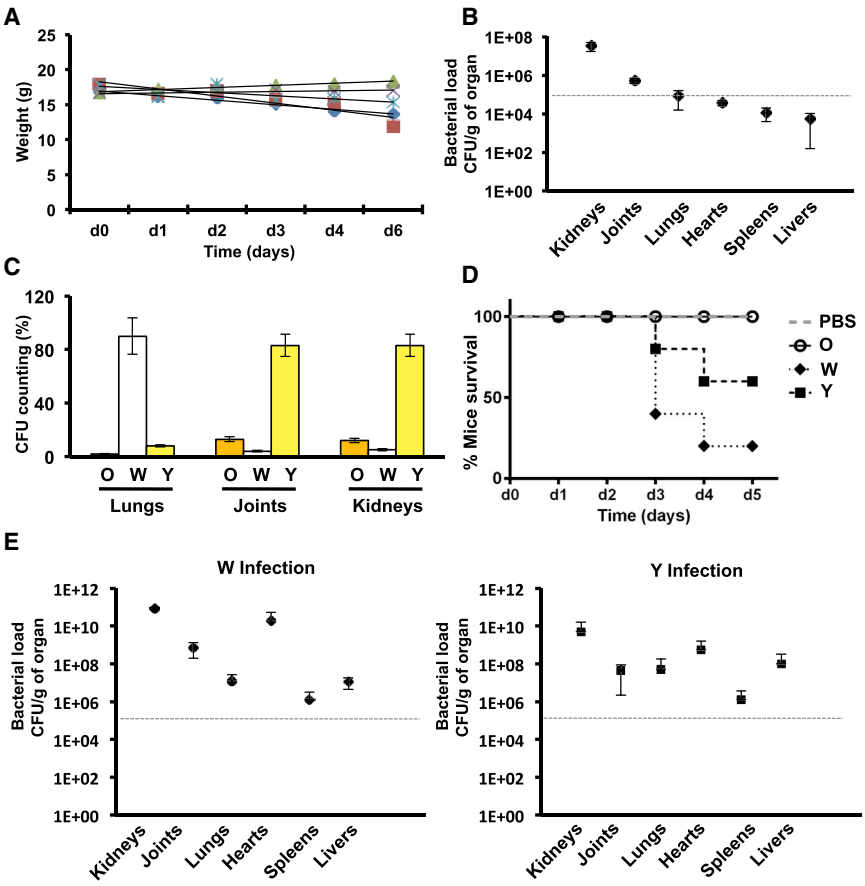

Figure 6. Diversification of *S. aureus* Communities In Vivo

(A) Weight loss of infected BALB/c mice (n = 5) during the course of the infection. Mice were infected with 10^7 SC01 derivative previously grown in TSB medium.

(B) Bacterial loads in the different organs counted as CFU/g of organ.

(C) Quantification of the CFU of the distinct strains in the organs that showed higher bacterial load ($\geq 10^5$ CFU/g).

(D) Survival curve of mice infected with O, W, or Y strains. Cohorts of five mice were infected with 10^7 cells (in the case of O, W, and Y infections) or PBS buffer as control. Mice were sacrificed when showing severe symptoms of infections (description of symptoms is in the Extended Experimental Procedures).

(E) Quantification of CFU/g of W and Y strains in the organs of infected mice. A gray, dashed line defines a cut-off number of 10^5 CFU/g to define high and low bacterial load.

See Table S7.

(Figure 6A), their organs collected, and the bacterial load counted and examined for strain diversification (Figure 6B). We detected low bacterial load ($\leq 10^5$ CFU/g) in livers, spleens, and hearts. Importantly, in these organs, the microbial community was a homogenous population of the parental O phenotype (data not shown). By contrast, the bacterial load in samples from the bones, lungs, and kidneys was higher ($\geq 10^5$ CFU/g) and contained a heterogeneous mixture of O, W, and Y cells (Figure 6C). Y was the most abundant strain collected from kidneys and bones, which are the two most important organs involved in magnesium homeostasis (Jahnen-Dechent, 2012). The lungs contained a higher proportion of W cells, which is consistent with the high number of σ^B-deficient strains generally isolated from lung infections (Karlsson-Kanth et al., 2006).

The O, W, and Y strains isolated from mice developed similar biofilm morphologies to the strains from the diversification experiments (Figure 7A). We tested three different W isolates from lungs (W_{m1}), bones (W_{m2}), and kidneys (W_{m3}) for their ability to spread, which occurred as previously described for the W strain (Figure 7B). Further qRT-PCR analyses verified the upregulation of RNAII and RNAIII and related genes (Figure 7C), which is consistent with a σ^B-deficient phenotype in the W_m strains. We sequenced the *sigB* operon in three different W_m isolates from each organ (lungs, bones, and kidneys). One bone isolate and one kidney isolate contained the same mutation in *rsbW* that was identified in our diversification experiment (D105N) (Figure S6A). A third bone isolate contained I11L mutation that generates an unstable SigB protein (Karlsson-Kanth et al., 2006) (Figure S6A). The other W_m strains contained an 11 bp deletion of the 5′ end of the *rsbU* gene, a frequently observed mutation known to confer a σ^B-deficient phenotype to diverse staphylococci (Herbert et al., 2010) (Figure S6A). Similarly, three different Y strains isolated from lungs (Y_{m1}), bones (Y_{m2}), and kidneys (Y_{m3}) displayed IR to vancomycin and lysostaphin treatment (Figure 7D). Further qRT-PCR analyses provided additional evidence for a gene expression profile consistent with a VISA-like phenotype (Figure 7E), and sequencing of *graRS*, *vraRS*, and *walKR* operons from three different Y_m isolates from lungs, bones, and kidneys detected several mutations in *graRS* and *vraRS* (Figure S6B). Altogether, these data provide multiple lines of evidence that strain diversification also occurs in vivo in a reproducible manner and generated similar phenotypes to those observed in the laboratory.

Finally, we compared the infective potential of the O, W, and Y strains that evolved in the laboratory experiment. To do this, two cohorts of five mice were infected with 10^7 W or Y cells previously grown in TSB medium, and the progression of the infection was monitored. Remarkably, we observed higher virulence in W and Y strains, manifested by the lower survival rate of infected mice in comparison to infections with the parental O strain (Figure 6D). The organs were collected, and their bacterial load was counted. Accordingly, high bacterial load ($\geq 10^5$ CFU/g) was detected in almost all organs, suggesting that, in contrast to the origin O strain, W or Y strains are more prone to give rise to severe bacteremia in our infection model (Figure 6E).

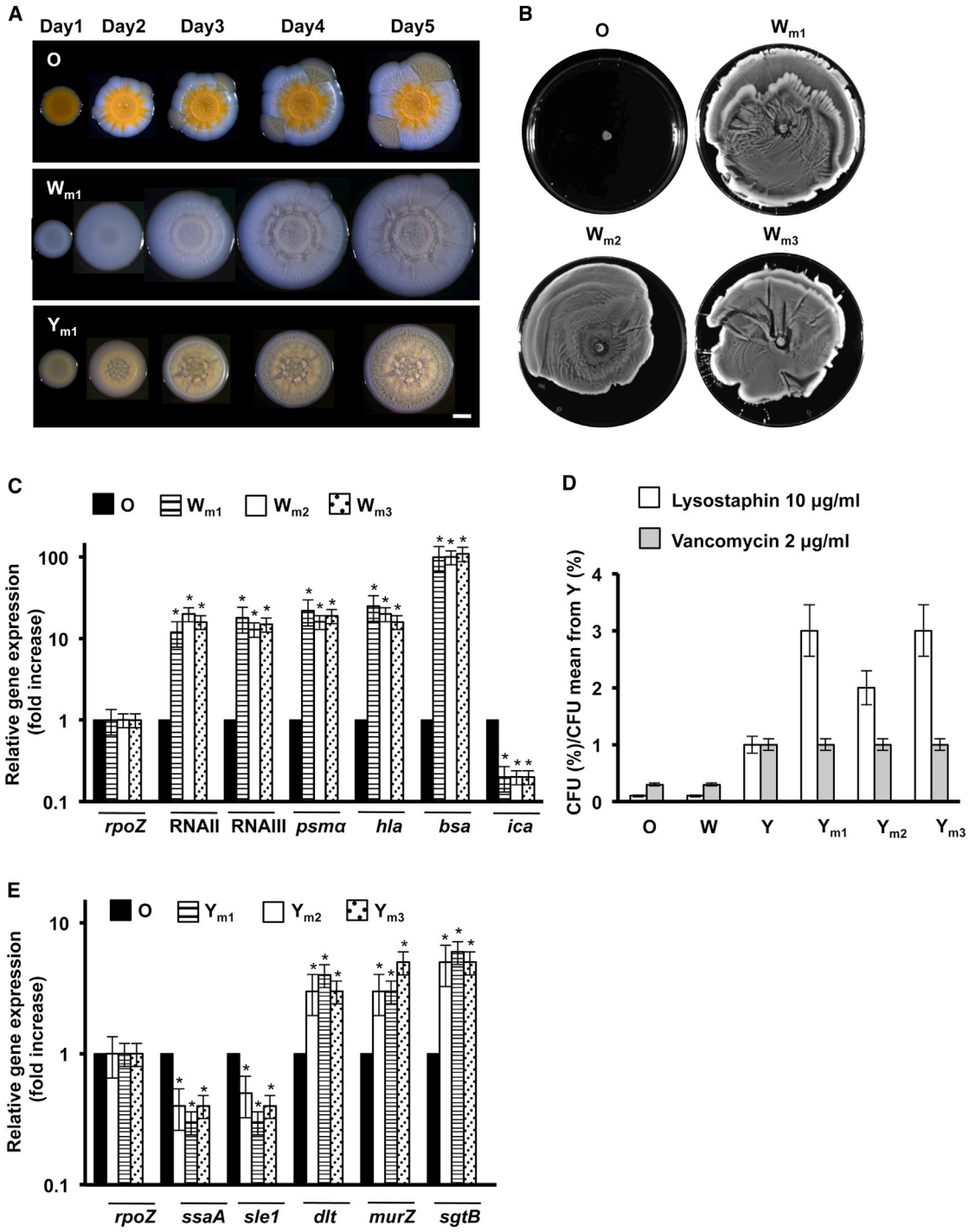

Figure 7. Adaptive Abilities of W_m and Y_m Strains Diversified In Vivo

(A) Progression of the O, W_m, and Y_m strains when growing in TSBMg for 5 days at 37°C. Scale bar, 1 mm.

(B) Spreading assay of distinct W_m strains.

(C) qRT-PCR of RNAII and RNAIII, RNAII-, and RNAIII-regulated genes *psmα* and *hla*, *bsa* and repressed *ica* gene.

(D) Quantification of bacterial survival in response to lysostaphin and vancomycin treatment of different Y_m strains. Values are presented in relation to Y strain.

(E) qRT-PCR analysis to monitor the differential expression of the VISA-related genes *ssaA* and *sle1* autolysins, *dltA*, and cell wall turnover *murZ* and *sgtB* genes (Student's t test, $p \leq 0.05$).

See Figures S6 and S7.

DISCUSSION

There is a growing recognition of the importance of social interactions for microbial communities (Nadell et al., 2009; West et al., 2006). Growth under biofilm-like conditions places cells in close proximity, which increases the potential for the phenotype of one cell to influence the evolution of other cells. In particular, there is often strong competition for resources and space that will favor strategies that enable one strain to suppress or outgrow another. Here, we have shown that these processes can have a major impact on one of the world's major pathogens. Growing CA-MRSA cells under biofilm-promoting conditions leads to an evolutionary arms race that begins when the W strain evolves and utilizes the increased secretion of PSMs and antibiotics to outcompete the WT O strain. However, the WT counter-adapts to this challenge and generates the Y strain that can resist the secreted products of W. Our assay utilizes a similar Mg^{2+} concentration to that found in tissues in which staphylococcal infections become chronic due to biofilm formation, such as bones (50 mM) or kidneys (30 mM) and is equivalent to other conventional assays (Beenken et al., 2003, 2004; Jahnen-Dechent, 2012). In addition to this, it is known that the sequestration of Mg^{2+} from tissues due to the use of tampons led to an outbreak of *S. aureus*-induced toxic shock syndrome in women in the USA (Schlievert, 1985). Given these correlations between Mg^{2+} and *S. aureus* infections, it is possible that Mg^{2+} acts upon the *agr* QS system that reciprocally regulates biofilm formation and the secretion of hemolytic toxins by a yet-unknown mechanism.

This assay revealed genetic diversification of a number of isolates, being especially evident in a CA-MRSA strain isolated from a hip wound (Tenover et al., 1994). The bone-associated origin of this strain is possibly relevant in its predisposition to diversify in our assay, which reflects the overwhelming inter-strain variation that exists within staphylococcal isolates (Herbert et al., 2010).

The evolved W and Y phenotypes resemble those seen in the clinics. σ^B-deficient strains such as the W strain are detected in 10% of staphylococcal infections (Lennette et al., 1985), and the Y phenotype closely resembles VISA strains, which are currently a major health problem, and suggests that VISA phenotypes can emerge in a manner that is unrelated to vancomycin treatment. Consistent with this, VISA strains have been observed in patients with renal failure or infections of a prosthetic joint that have not received vancomycin (Charles et al., 2004; Howden et al., 2010; Jahnen-Dechent, 2012). Our work suggests that competition within biofilms can be central to understanding pathogenic phenotypes and emphasizes the need to consider not only the impact of treatment of bacterial infections but also the interactions among the bacteria themselves.

EXPERIMENTAL PROCEDURES

Strains, Media, and Culture Conditions

The strain used for diversification was *S. aureus* derivative of Sc01 (Beenken et al., 2003). Complete strain and plasmid lists are shown in Tables S1 and S2. For biofilm formation in agar, an inoculum TSB plate was grown for 12 hr at 37°C. 2 μl of a cell suspension was spotted on the surface of TSBMg and incubated at 37°C for 5 days. When specified, 5 μM AIP was added. Bsa was added to different concentrations that are specified in the paper. Specific growth conditions are presented in figure legends.

Conventional liquid-surface biofilm formation assays were performed in TSB + glucose 0.5% + NaCl 3% (Beenken et al., 2003; Götz, 2002). Secretion of hemolytic toxins was monitored by spotting 3 μl of cultures in TSB 5% blood agar plates and measuring the diameter size after incubating at 37°C for 24 hr. A protocol for staphyloxanthin purification was obtained from Pelz et al. (2005). To assay spreading on solid surfaces, 2 μl of an overnight culture was spotted on TSB 0.24% agar plates and incubated at 37°C for 24 hr (Tsompanidou et al., 2011). To assess resistance of cells to lysostaphin, cells were resuspended in 1 ml PBS and incubated for 15 min at 37°C in the presence of lysostaphin (10 μg/ml) (Cui et al., 2006) prior to dilution plating on TSB agar to determine CFU/ml.

RNA Extraction and Analysis

O, W, and Y cultures were resuspended in RNA Protect (QIAGEN) and were mechanically lysed using glass beads in a Fast Prep Shaker (two times; 45 s; speed, 6.5). The supernatants were used for RNA isolation using the RNeasy mini kit (QIAGEN). The isolated RNA was treated with RNase-free DNase I to remove DNA traces. The cDNA libraries were generated as described previously but omitting the RNA size-fractionation step prior to cDNA synthesis (Dugar et al., 2013). The libraries were sequenced with an Illumina HiSeq machine with 100 cycles in single end mode. The demultiplexed files and coverages files have been deposited in NCBI's GEO database (GSE49636). For qRT-PCR analysis, total RNA was reverse transcribed using hexameric random primers, followed by qRT-PCR using SsoAdvanced SYBR Green Supermix (BioRad) (primers listed in Table S2).

Mouse Infection Studies

All animal studies were approved by the local government of Franconia, Germany (license number 55.2-2531.01-06/12) and performed in strict accordance with the guidelines for animal care and experimentation. We used female BALB/c mice (16–18 g) (Charles River). *S. aureus* was cultured for 18 hr at 37°C on a TSB plate. Cells were diluted to the desired concentration and validated by dilution plating in TSB agar. 100 μl *S. aureus* culture was injected into the tail vein. 6 days after bacterial challenge, organs were aseptically harvested and the CFU determined. Organs were homogenized in 2 ml of sterile PBS using Dispomix (Bio-Budget Technologies GmbH). Joints were ground in a mortar prior homogenization. Serial dilutions of each organ were plated on mannitol salt-phenol red agar plates and TSB plates and incubated at 37°C for at least 48 hr. CFUs were counted, and the bacterial burden was calculated as CFU/g of organ. To compare the infective potential of O, W, and Y strains, three cohorts of five mice were infected with 100 μl *S. aureus* culture containing 10^7 cells injected into the tail vein. The infections were allowed to progress until severe infections symptoms occurred or to an endpoint of 5 days. Organs were aseptically harvested, and the CFU was determined.

ACCESSION NUMBERS

The demultiplexed files and coverages files have been deposited in NCBI's GEO database under the accession number GSE49636.

SUPPLEMENTAL INFORMATION

Supplemental Information includes Extended Experimental Procedures, seven figures, and seven tables and can be found with this article online at http://dx.doi.org/10.1016/j.cell.2014.06.046.

ACKNOWLEDGMENTS

We thank IMIB, especially Stan Gorski for his help in editing the manuscript, Dr. S. Engelmann (Univ. Greifswald, Germany) for providing antibodies, and AG Ohlsen for guidance with animal experiments. This work was funded by ZINF (D.L.); the DFG grants LO 1804/2-1 (D.L.) and SFB-TR34 Z3 (K.O.); and ERC grants 242670 (K.R.F.) and 335568 (D.L.). G.K. is a recipient of FWF fellowship.

Received: January 25, 2014
Revised: April 28, 2014
Accepted: June 23, 2014
Published: August 28, 2014

REFERENCES

Allen, H.K., Donato, J., Wang, H.H., Cloud-Hansen, K.A., Davies, J., and Handelsman, J. (2010). Call of the wild: antibiotic resistance genes in natural environments. Nat. Rev. Microbiol. *8*, 251–259.

Beenken, K.E., Blevins, J.S., and Smeltzer, M.S. (2003). Mutation of sarA in *Staphylococcus aureus* limits biofilm formation. Infect. Immun. *71*, 4206–4211.

Beenken, K.E., Dunman, P.M., McAleese, F., Macapagal, D., Murphy, E., Projan, S.J., Blevins, J.S., and Smeltzer, M.S. (2004). Global gene expression in *Staphylococcus aureus* biofilms. J. Bacteriol. *186*, 4665–4684.

Benveniste, R., and Davies, J. (1973). Aminoglycoside antibiotic-inactivating enzymes in actinomycetes similar to those present in clinical isolates of antibiotic-resistant bacteria. Proc. Natl. Acad. Sci. USA *70*, 2276–2280.

Bischoff, M., Entenza, J.M., and Giachino, P. (2001). Influence of a functional sigB operon on the global regulators sar and agr in *Staphylococcus aureus*. J. Bacteriol. *183*, 5171–5179.

Bischoff, M., Dunman, P., Kormanec, J., Macapagal, D., Murphy, E., Mounts, W., Berger-Bächi, B., and Projan, S. (2004). Microarray-based analysis of the *Staphylococcus aureus* sigmaB regulon. J. Bacteriol. *186*, 4085–4099.

Boles, B.R., and Horswill, A.R. (2008). Agr-mediated dispersal of Staphylococcus aureus biofilms. PLoS Pathog. *4*, e1000052.

Branda, S.S., González-Pastor, J.E., Ben-Yehuda, S., Losick, R., and Kolter, R. (2001). Fruiting body formation by *Bacillus subtilis*. Proc. Natl. Acad. Sci. USA *98*, 11621–11626.

Brown, D.R., and Pattee, P.A. (1980). Identification of a chromosomal determinant of alpha-toxin production in *Staphylococcus aureus*. Infect. Immun. *30*, 36–42.

Camargo, I.L., Neoh, H.M., Cui, L., and Hiramatsu, K. (2008). Serial daptomycin selection generates daptomycin-nonsusceptible *Staphylococcus aureus* strains with a heterogeneous vancomycin-intermediate phenotype. Antimicrob. Agents Chemother. *52*, 4289–4299.

Cantón, R., and Morosini, M.-I. (2011). Emergence and spread of antibiotic resistance following exposure to antibiotics. FEMS Microbiol. Rev. *35*, 977–991.

Charles, P.G.P., Ward, P.B., Johnson, P.D.R., Howden, B.P., and Grayson, M.L. (2004). Clinical features associated with bacteremia due to heterogeneous vancomycin-intermediate *Staphylococcus aureus*. Clin. Infect. Dis. *8*, 448–451.

Cui, L., Iwamoto, A., Lian, J.Q., Neoh, H.M., Maruyama, T., Horikawa, Y., and Hiramatsu, K. (2006). Novel mechanism of antibiotic resistance originating in vancomycin-intermediate *Staphylococcus aureus*. Antimicrob. Agents Chemother. *50*, 428–438.

Daly, K.M., Upton, M., Sandiford, S.K., Draper, L.A., Wescombe, P.A., Jack, R.W., O'Connor, P.M., Rossney, A., Götz, F., Hill, C., et al. (2010). Production of the Bsa lantibiotic by community-acquired *Staphylococcus aureus* strains. J. Bacteriol. *192*, 1131–1142.

Diep, B.A., Chambers, H.F., Graber, C.J., Szumowski, J.D., Miller, L.G., Han, L.L., Chen, J.H., Lin, F., Lin, J., Phan, T.H., et al. (2008). Emergence of multidrug-resistant, community-associated, methicillin-resistant *Staphylococcus aureus* clone USA300 in men who have sex with men. Ann. Intern. Med. *148*, 249–257.

Dufour, A., and Haldenwang, W.G. (1994). Interactions between a *Bacillus subtilis* anti-sigma factor (RsbW) and its antagonist (RsbV). J. Bacteriol. *176*, 1813–1820.

Dugar, G., Herbig, A., Förstner, K.U., Heidrich, N., Reinhardt, R., Nieselt, K., and Sharma, C.M. (2013). High-resolution transcriptome maps reveal strain-specific regulatory features of multiple *Campylobacter jejuni* isolates. PLoS Genet. *9*, e1003495.

Götz, F. (2002). *Staphylococcus* and biofilms. Mol. Microbiol. *43*, 1367–1378.

Graham, J.W., Lei, M.G., and Lee, C.Y. (2013). Trapping and identification of cellular substrates of the *Staphylococcus aureus* ClpC chaperone. J. Bacteriol. *195*, 4506–4516.

Günther, T. (2011). Magnesium in bone and the magnesium load test. Magnes. Res. *24*, 223–224.

Hafer, C., Lin, Y., Kornblum, J., Lowy, F.D., and Uhlemann, A.C. (2012). Contribution of selected gene mutations to resistance in clinical isolates of vancomycin-intermediate *Staphylococcus aureus*. Antimicrob. Agents Chemother. *56*, 5845–5851.

Herbert, S., Ziebandt, A.K., Ohlsen, K., Schäfer, T., Hecker, M., Albrecht, D., Novick, R., and Götz, F. (2010). Repair of global regulators in *Staphylococcus aureus* 8325 and comparative analysis with other clinical isolates. Infect. Immun. *78*, 2877–2889.

Hibbing, M.E., Fuqua, C., Parsek, M.R., and Peterson, S.B. (2010). Bacterial competition: surviving and thriving in the microbial jungle. Nat. Rev. Microbiol. *8*, 15–25.

Hiramatsu, K., Hanaki, H., Ino, T., Yabuta, K., Oguri, T., and Tenover, F.C. (1997). Methicillin-resistant *Staphylococcus aureus* clinical strain with reduced vancomycin susceptibility. J. Antimicrob. Chemother. *40*, 135–136.

Howden, B.P., Davies, J.K., Johnson, P.D.R., Stinear, T.P., and Grayson, M.L. (2010). Reduced vancomycin susceptibility in *Staphylococcus aureus*, including vancomycin-intermediate and heterogeneous vancomycin-intermediate strains: resistance mechanisms, laboratory detection, and clinical implications. Clin. Microbiol. Rev. *23*, 99–139.

Jahnen-Dechent, W.K.M. (2012). Magnesium basics. Clin. Kidney J. *5*, 2.

Karlsson-Kanth, A., Tegmark-Wisell, K., Arvidson, S., and Oscarsson, J. (2006). Natural human isolates of *Staphylococcus aureus* selected for high production of proteases and alpha-hemolysin are sigmaB deficient. Int. J. Med. Microbiol. *296*, 229–236.

Kies, S., Vuong, C., Hille, M., Peschel, A., Meyer, C., Götz, F., and Otto, M. (2003). Control of antimicrobial peptide synthesis by the agr quorum sensing system in *Staphylococcus epidermidis*: activity of the lantibiotic epidermin is regulated at the level of precursor peptide processing. Peptides *24*, 329–338.

Klevens, R.M., Morrison, M.A., Nadle, J., Petit, S., Gershman, K., Ray, S., Harrison, L.H., Lynfield, R., Dumyati, G., Townes, J.M., et al.; Active Bacterial Core surveillance (ABCs) MRSA Investigators (2007). Invasive methicillin-resistant *Staphylococcus aureus* infections in the United States. JAMA *298*, 1763–1771.

Kluytmans, J., van Belkum, A., and Verbrugh, H. (1997). Nasal carriage of *Staphylococcus aureus*: epidemiology, underlying mechanisms, and associated risks. Clin. Microbiol. Rev. *10*, 505–520.

Kos, V.N., Desjardins, C.A., Griggs, A., Cerqueira, G., Van Tonder, A., Holden, M.T., Godfrey, P., Palmer, K.L., Bodi, K., Mongodin, E.F., et al. (2012). Comparative genomics of vancomycin-resistant *Staphylococcus aureus* strains and their positions within the clade most commonly associated with Methicillin-resistant S. aureus hospital-acquired infection in the United States. mBio. *3*, e00112.

Kreiswirth, B., Kornblum, J., Arbeit, R.D., Eisner, W., Maslow, J.N., McGeer, A., Low, D.E., and Novick, R.P. (1993). Evidence for a clonal origin of methicillin resistance in *Staphylococcus aureus*. Science *259*, 227–230.

Kullik, I., Giachino, P., and Fuchs, T. (1998). Deletion of the alternative sigma factor sigmaB in Staphylococcus aureus reveals its function as a global regulator of virulence genes. J. Bacteriol. *180*, 4814–4820.

Lennette E.H., Balows A., Hausler W.J., Jr., and Shadomy H.J., eds. Manual of Clinical Microbiology (Washington, D.C.: American Society for Microbiology).

López, D., Vlamakis, H., and Kolter, R. (2010). Biofilms. Cold Spring Harb. Perspect. Biol. *2*, a000398.

Marles-Wright, J., and Lewis, R.J. (2010). The stressosome: molecular architecture of a signalling hub. Biochem. Soc. Trans. *38*, 928–933.

Marshall, J.H., and Wilmoth, G.J. (1981). Proposed pathway of triterpenoid carotenoid biosynthesis in *Staphylococcus aureus*: evidence from a study of mutants. J. Bacteriol. *147*, 914–919.

Matsuo, M., Cui, L., Kim, J., and Hiramatsu, K. (2013). Comprehensive identification of mutations responsible for heterogeneous vancomycin-intermediate *Staphylococcus aureus* (hVISA)-to-VISA conversion in laboratory-generated VISA strains derived from hVISA clinical strain Mu3. Antimicrob. Agents Chemother. *57*, 5843–5853.

MDowell, P., Affas, Z., Reynolds, C., Holden, M.T., Wood, S.J., Saint, S., Cockayne, A., Hill, P.J., Dodd, C.E., Bycroft, B.W., et al. (2001). Structure, activity and evolution of the group I thiolactone peptide quorum-sensing system of *Staphylococcus aureus*. Mol. Microbiol. *41*, 503–512.

Morfeldt, E., Taylor, D., von Gabain, A., and Arvidson, S. (1995). Activation of alpha-toxin translation in *Staphylococcus aureus* by the trans-encoded antisense RNA, RNAIII. EMBO J. *14*, 4569–4577.

Morfeldt, E., Tegmark, K., and Arvidson, S. (1996). Transcriptional control of the agr-dependent virulence gene regulator, RNAIII, in *Staphylococcus aureus*. Mol. Microbiol. *21*, 1227–1237.

Nadell, C.D., Xavier, J.B., and Foster, K.R. (2009). The sociobiology of biofilms. FEMS Microbiol. Rev. *33*, 206–224.

Novick, R.P., and Geisinger, E. (2008). Quorum sensing in staphylococci. Annu. Rev. Genet. *42*, 541–564.

O'Gara, J.P. (2007). ica and beyond: biofilm mechanisms and regulation in Staphylococcus epidermidis and *Staphylococcus aureus*. FEMS Microbiol. Lett. *270*, 179–188.

Otto, M. (2008). Staphylococcal biofilms. Curr. Top. Microbiol. Immunol. *322*, 207–228.

Otto, M. (2012). MRSA virulence and spread. Cell. Microbiol. *14*, 1513–1521.

Peleg, A.Y., Miyakis, S., Ward, D.V., Earl, A.M., Rubio, A., Cameron, D.R., Pillai, S., Moellering, R.C., Jr., and Eliopoulos, G.M. (2012). Whole genome characterization of the mechanisms of daptomycin resistance in clinical and laboratory derived isolates of *Staphylococcus aureus*. PLoS ONE *7*, e28316.

Pelz, A., Wieland, K.P., Putzbach, K., Hentschel, P., Albert, K., and Götz, F. (2005). Structure and biosynthesis of staphyloxanthin from *Staphylococcus aureus*. J. Biol. Chem. *280*, 32493–32498.

Peng, H.L., Novick, R.P., Kreiswirth, B., Kornblum, J., and Schlievert, P. (1988). Cloning, characterization, and sequencing of an accessory gene regulator (agr) in *Staphylococcus aureus*. J. Bacteriol. *170*, 4365–4372.

Pereira, P.M., Filipe, S.R., Tomasz, A., and Pinho, M.G. (2007). Fluorescence ratio imaging microscopy shows decreased access of vancomycin to cell wall synthetic sites in vancomycin-resistant *Staphylococcus aureus*. Antimicrob. Agents Chemother. *51*, 3627–3633.

Queck, S.Y., Jameson-Lee, M., Villaruz, A.E., Bach, T.-H.L., Khan, B.A., Sturdevant, D.E., Ricklefs, S.M., Li, M., and Otto, M. (2008). RNAIII-independent target gene control by the agr quorum-sensing system: insight into the evolution of virulence regulation in *Staphylococcus aureus*. Mol. Cell *32*, 150–158.

Recsei, P., Kreiswirth, B., O'Reilly, M., Schlievert, P., Gruss, A., and Novick, R.P. (1986). Regulation of exoprotein gene expression in *Staphylococcus aureus* by agar. Mol. Gen. Genet. *202*, 58–61.

Schlievert, P.M. (1985). Effect of magnesium on production of toxic-shock-syndrome toxin-1 by *Staphylococcus aureus*. J. Infect. Dis. *152*, 618–620.

Serra, D.O., Richter, A.M., Klauck, G., Mika, F., and Hengge, R. (2013). Microanatomy at cellular resolution and spatial order of physiological differentiation in a bacterial biofilm. mBio *4*, e00103–e00113.

Servin-Massieu, M. (1961). Spontaneous appearance of sectored colonies in *Staphylococcus aureus* cultures. J. Bacteriol. *82*, 316–317.

Sieradzki, K., and Tomasz, A. (2003). Alterations of cell wall structure and metabolism accompany reduced susceptibility to vancomycin in an isogenic series of clinical isolates of *Staphylococcus aureus*. J. Bacteriol. *185*, 7103–7110.

Tenover, F.C., Arbeit, R., Archer, G., Biddle, J., Byrne, S., Goering, R., Hancock, G., Hébert, G.A., Hill, B., Hollis, R., et al. (1994). Comparison of traditional and molecular methods of typing isolates of *Staphylococcus aureus*. J. Clin. Microbiol. *32*, 407–415.

Thoendel, M., Kavanaugh, J.S., Flack, C.E., and Horswill, A.R. (2011). Peptide signaling in the staphylococci. Chem. Rev. *111*, 117–151.

Tsompanidou, E., Sibbald, M.J., Chlebowicz, M.A., Dreisbach, A., Back, J.W., van Dijl, J.M., Buist, G., and Denham, E.L. (2011). Requirement of the agr locus for colony spreading of *Staphylococcus aureus*. J. Bacteriol. *193*, 1267–1272.

Tsompanidou, E., Denham, E.L., Becher, D., de Jong, A., Buist, G., van Oosten, M., Manson, W.L., Back, J.W., van Dijl, J.M., and Dreisbach, A. (2013). Distinct roles of phenol-soluble modulins in spreading of *Staphylococcus aureus* on wet surfaces. Appl. Environ. Microbiol. *79*, 886–895.

Votintseva, A.A., Miller, R.R., Fung, R., Knox, K., Godwin, H., Peto, T.E., Crook, D.W., Bowden, R., and Walker, A.S. (2014). Multiple-strain colonization in nasal carriers of *Staphylococcus aureus*. J. Clin. Microbiol. *52*, 1192–1200.

West, S.A., Griffin, A.S., Gardner, A., and Diggle, S.P. (2006). Social evolution theory for microorganisms. Nat. Rev. Microbiol. *4*, 597–607.